Improved HDDR processing route for production of anisotropic powder from sintered NdFeB type magnets

Sheridan, Richard; Williams, A.J; Harris, Ivor; Walton, A.

[Link to publication on Research at Birmingham portal](#)

Improved HDDR processing route for production of anisotropic powder from sintered NdFeB type magnets

R.S. Sheridan, A.J. Williams, I.R. Harris, A. Walton [*]

School of Metallurgy and Materials, University of Birmingham, Edgbaston, Birmingham B15 2TT, United Kingdom

A B S T R A C T

The hydrogenation disproportionation desorption recombination (HDDR) process has been investigated as a possible means of producing bonded magnets from used NdFeB-type sintered magnets with compositions, $Nd_{13.4}Dy_{0.8}Al_{0.7}Nb_{0.3}Fe_{78.5}B_{6.3}$ and $Nd_{12.5}Dy_{1.8}Al_{0.9}Nb_{0.6}Co_{5.0}Fe_{72.8}B_{6.4}$ (atomic%). It has been shown that by increasing the processing temperature, an increase in the equilibrium pressure for disproportionation and in the overall reaction time was observed. The magnetic properties of the lower Dy content magnet were affected significantly by the change in processing temperature with a peak in properties observed at 880 °C producing magnetic powder with a remanence of 1.08 (± 0.02) T, a coercivity of 840 (± 17) kA m^{-1}, and a maximum energy product of 175 (± 2.5) kJ m^{-3}. Further work on magnets with a significantly higher Dy content has shown that simultaneous processing of sintered magnets with varying compositions can be achieved by increasing the hydrogen pressure, however a range of magnetic properties are produced depending on the initial compositions of the samples in the input feed.

1. Introduction

Neodymium-iron-boron (NdFeB) magnets have become an integral part of many electrical components since their development in 1984 [1,2]. NdFeB magnets are used in applications such as hard-disk drives, permanent magnet motors (e.g. in hybrid vehicles) and more recently in generators for large offshore wind turbines.

China currently supplies over 95% of rare earth materials to the world market including Nd, Pr and Dy which are used in NdFeB-based magnets. However, in recent years, China imposed export quotas for these materials and in 2010 this was cut by around 40%. This resulted in dramatic price fluctuations for these materials in world markets which has placed considerable strain on the manufacturers and end users of NdFeB-based magnets.

Fortunately, there are alternative sources of rare earths worldwide and mines are opening in, for instance, Australia, USA and South Africa. However, the start-up time for a new mine can be considerable and the extraction processes used to separate the individual rare earths are complicated and energy intensive. Recycling of magnets contained within redundant electrical equipment could provide a secure and alternative supply of these materials.

It has been reported [3,4] that hydrogen can be used as an effective method of recycling NdFeB by utilising the hydrogen decrepitation (HD) process to turn solid sintered magnets into a demagnetised powder for further processing [3]. The HD process has also been used as a way of separating used NdFeB magnets from hard disk drive assemblies [3–8]. The present findings form just a small part of an extensive research programme into the use of hydrogen for recycling of NdFeB-type magnets at the University of Birmingham.

It has been shown that the powder produced after HD treating sintered NdFeB magnets can be re-sintered successfully to produce high density magnets with magnetic properties comparable to those of the starting material [3,9]. Alternatively, the HD powder could be processed further by using the hydrogenation, disproportionation, desorption, recombination, (HDDR) process [10,11]. This process utilises hydrogen at elevated temperatures to refine the grain size to ∼0.3 μm [12–14], allowing more grains per particle and hence an increased coercivity and corrosion resistance.

Most previous work undertaken on HDDR processing of sintered NdFeB magnets has led to the production of magnetically isotropic powder [15,16], which leads to a significant reduction in the remanence of the powder. The production of anisotropic HDDR powder from cast starting material has been reported from many sources [13]. However, this has been achieved mostly by introducing additions of cobalt, gallium, zirconium or niobium to alter the kinetics of the HDDR process. Alternatively, it has been shown that anisotropic powder can be produced by careful control of the

hydrogen pressure under certain conditions during the HDDR process, without the requirement for kinetic-altering additions [14,17]. Nakamura et al. [18] and Sugimoto et al. [19] showed that, by heating cast NdFeB in vacuum prior to the introduction of hydrogen (termed v-HD treatment), it is possible to prevent disproportionation of the powder until the required processing temperature is attained. Following the disproportionation stage, the hydrogen pressure is reduced to encourage desorption of hydrogen from the sample which results in the recombination reaction. This recombination can either be induced by manually lowering the hydrogen pressure using a rotary vacuum pump or by flushing with argon as demonstrated in the s-DR process [18,19].

The present authors have shown previously [20] that it is possible to produce anisotropic powder from sintered material under a specific set of processing conditions, resulting in reasonable permanent magnetic properties and other authors have followed on from this to investigate different compositions [21]. In the present work, the HDDR process is initiated after the HD process is complete. The HD powder is degassed by heating under vacuum to the required processing temperature where hydrogen is slowly introduced to encourage disproportionation at a slow rate. The HDDR reaction equation can be described as

Disproportionation →

$$Nd_2Fe_{14}B + 2xH_2 \leftrightarrow 2NdH_{2x} + 12Fe + Fe_2B$$
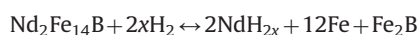
← Recombination

where x approaches 1.0 at elevated temperatures.

The work presented in this paper shows how these processes can be applied in the reprocessing of scrap sintered magnets. This paper is an extension of previous work [20,22] combining the use of a higher processing pressure during disproportionation and avoiding subsequent oxygen exposure by performing both the HD and HDDR processes in the same furnace, thus avoiding intermediate exposure to the atmosphere. The processing conditions for mixed batches of materials are also investigated.

2. Materials and methods

Uncoated scrap sintered magnets were used throughout this study. Ion coupled plasma (ICP) spectroscopy was used to determine the composition of the two types of magnets. Composition 1 was identified as $Nd_{13.4}Dy_{0.8}Al_{0.7}Nb_{0.3}Fe_{78.5}B_{6.3}$ (atomic%) with an oxygen content of 4300 ppm. The magnetic properties were: remanence, 1.36 (± 0.02) T, intrinsic coercivity, 860 (± 17) kA m^{-1} and a maximum energy product of 340 (± 2.5) kJ m^{-3}.

Composition 2 was shown to be $Nd_{12.5}Dy_{1.8}Al_{0.9}Nb_{0.6}Co_{5.0}$-$Fe_{72.8}B_{6.4}$ (atomic%) with an oxygen content of 4130 ppm, the magnetic properties of which were: remanence, 1.1 (± 0.02) T, intrinsic coercivity, > 1450 kA m^{-1} and a maximum energy product of > 230 kJ m^{-3}.

The magnetic properties of these starting magnets were determined using a permeameter, but it was not possible to fully demagnetise the sample with composition 2, due to the limited field of the current equipment. Hence only approximate values of the coercivity and the maximum energy product are quoted here.

The sintered blocks of both magnet compositions were broken into pieces and 20 g was loaded into a stainless steel tube, and then placed inside an Inconel-tube furnace. The system was evacuated using a rotary pump (to $\sim 10^{-2}$ mbar) and the sintered magnet pieces were then hydrogen decrepitated using a pressure of 2 bar of hydrogen at room temperature to produce a hydrided powder. The system was subsequently evacuated and the sample heated under vacuum at a rate of 800 °C h^{-1}, to a temperature T, which varied from 830 to 930 °C and the hydrogen desorption

trace was measured using a Lesker vacuum gauge with attached data logger to monitor the pressure in the furnace tube and the temperature of the sample. When the desired process temperature (T) was attained, hydrogen was introduced at a rate 16 mbar min^{-1} to the processing pressure of 1500 mbar and then held for 30 min, giving an overall processing time of roughly 2 h. The hydrogen pressure was then reduced at a rate of 100 mbar min^{-1} until the pressure reached that of the rotary pump vacuum and the sample was then cooled quickly by rolling the furnace off the tube and placing a water-cooled copper coil over the tube. By this means, cooling of the powder to below 500 °C occurred in less than 5 min, thus preventing excessive grain growth at elevated temperatures. These conditions are shown in the schematic in Fig. 1.

For the mixed batch processing of samples with compositions 1 and 2, the processing temperature was set to 880 °C and the disproportionation stage was altered by ramping at 16 mbar min^{-1} to 2000 mbar but not held, thus maintaining a disproportionation time of 2 h. These amended processing conditions are shown schematically in Fig. 2.

Once cooled, the samples were removed from the furnace, lightly ground using a pestle and mortar to break up any agglomerated powder and then prepared for testing.
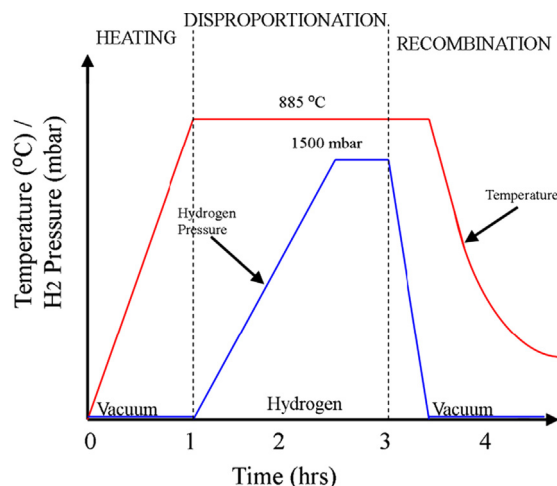

Fig. 1. Schematic showing the HDDR processing conditions for sample with composition 1.
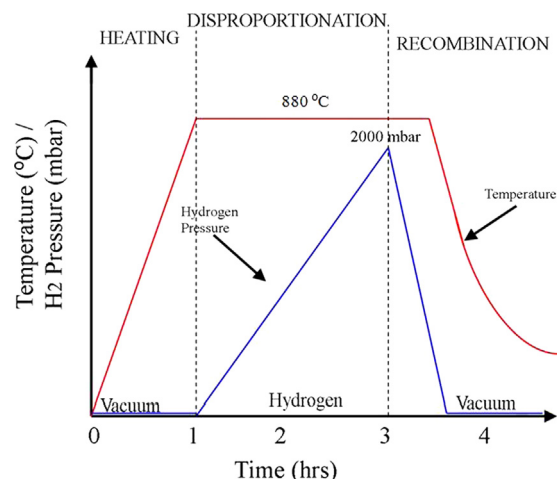

Fig. 2. Schematic showing HDDR processing conditions for mixed batch processing of samples with compositions 1 and 2.

Powder samples of ~100 mg were set in wax in cylindrical sample holders and aligned using a constant 1.7T field from a permeameter electromagnet in order to align the particles in the preferential c-axis direction. Once set, the samples were pulse magnetised in the c-axis direction, using a field of 4 T from a capacitor discharge pulse magnetiser. The samples were subsequently measured magnetically using a Lakeshore 7300 Vibrating Sample Magnetometer (VSM) in both the "easy" direction (parallel to the c-axis) and the "hard" direction (perpendicular to the c-axis). The specific magnetisation values of the VSM were converted to polarisation values using a theoretical density of 7.5 g cm^{-3}. There was no attempt to predict a self-demagnetisation factor for the measurements due to the wide variation in the particle shapes and sizes, hence the magnetic properties remain uncorrected.

3. Results and discussion

Composition 1 was HDDR processed as described in the experimental section. By performing the HD and HDDR reactions within the same vessel this has reduced markedly the opportunity for surface reactions with the atmosphere during the transfer of the HD-treated powder samples into the HDDR rig. During heating of the sample under vacuum in the initial stage of the HDDR process, the hydrogen absorbed during the HD process is desorbed and the change in pressure within the HDDR vessel, associated with this desorption, is recorded and plotted against temperature (Fig. 3.)

The large initial peak, labelled A, is associated with a combination of the desorption of hydrogen from the $Nd_2Fe_{14}B$ matrix phase and the desorption that occurs during the transformation of $NdH_{2.7}$ to NdH_2 in the Nd-rich material. The second peak, labelled B, is due to the desorption of hydrogen from NdH_2 which transforms to Nd as demonstrated by Williams et al. (1991) [23] during hydrogen desorption studies using mass spectrometry.

For composition 1, this desorption trace is reproducible as demonstrated by the overlapping traces for the two samples shown in Fig. 3.

During the disproportionation stage, hydrogen is again absorbed by the sample as soon as the pressure reaches the equilibrium point, at which time it drives the system to the right hand side of Equation 1. The hydrogen absorption behaviour is monitored using a mass flow controller until disproportionation is complete, as shown in Fig. 4.

Fig. 4 shows that, as the processing temperature is increased, the hydrogen pressure required to initiate disproportionation is increased. Another trend is that, with increasing temperature, the
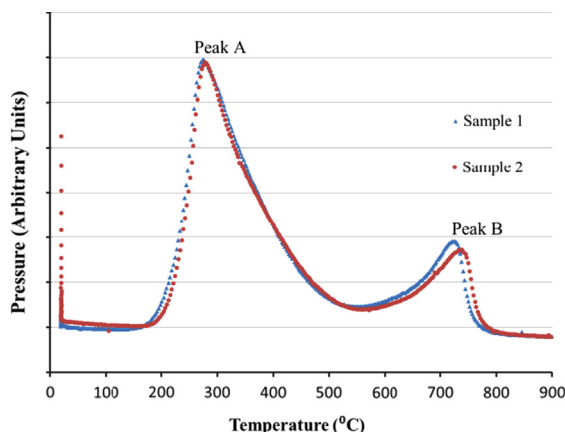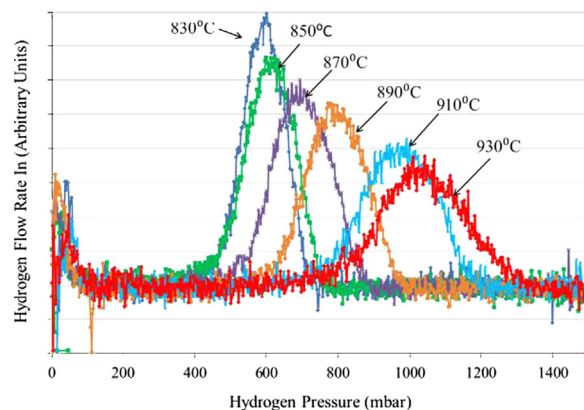

Fig. 4. Comparison of disproportionation absorption peaks of a sample of composition 1 with increasing processing temperature.
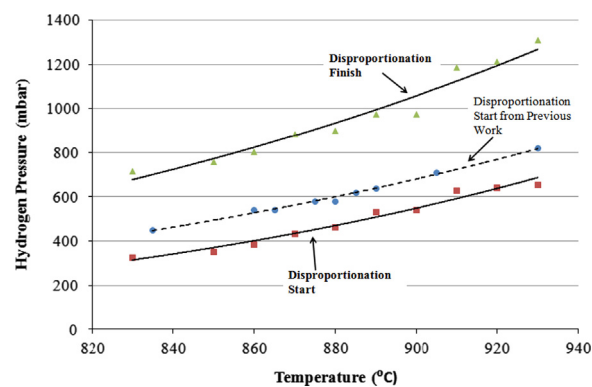

Fig. 5. Variation of disproportionation start and finish points with respect to temperature for samples of composition 1.

peak height is reduced but the overall peak width is broadened, indicating that it takes longer for completion of the reaction. This can be attributed to the decreased stability of NdH2 at elevated temperatures. By using a processing pressure of 1500 mbar of hydrogen, all of the samples were able to completely disproportionate during the pressure ramp stage, thus allowing a comparison of the start and finish points, as observed in Fig. 5.

Fig. 5 shows that the disproportionation start points are significantly lower with the present, improved processing conditions when compared with those reported in the previous work [20]. For example, in the previous work the disproportionation start point for the sample processed at 880 °C was 585 mbar, whereas using the improved conditions resulted in the disproportionation start point of 464 mbar. This represents a reduction of ~21%.

The significantly lower start pressures can be attributed to the absence of reaction products at the grain boundaries and triple points such as Nd_2O_3 and $Nd(OH)_3$, formed on exposure to atmospheric conditions [24] (which will contain water) during loading of the sample into the HDDR rig. This has now been avoided by performing the HD and HDDR processes in the same sealed Inconel tube furnace. It can be deduced that these reaction products impede the absorption of hydrogen by the Nd-rich grain boundary phase, which has been shown to act as a path to the subsequent disproportionation of the matrix $Nd_2Fe_{14}B$ phase [25].

However, the reaction finish points are almost identical for those that finish below 1000 mbar.

The effects of varying the processing temperature on the magnetic properties of the samples are shown in Fig. 6.
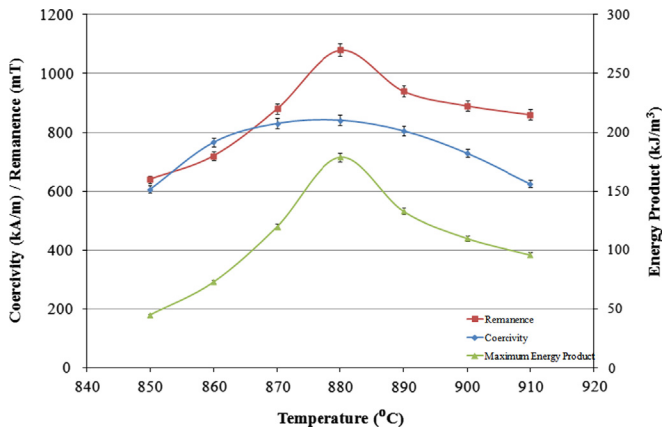

Fig. 3. Desorption trace for two identical HD-treated samples of composition 1, degassed during heating.

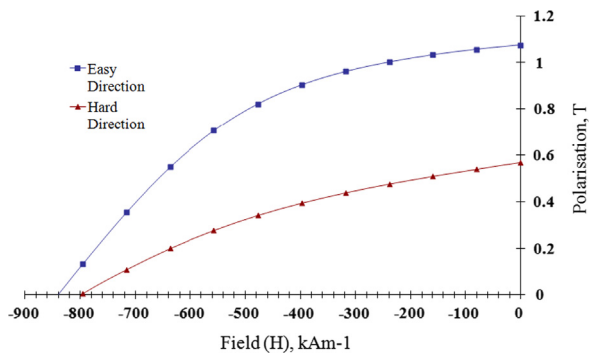Fig. 6. Variation of coercivity, remanence and energy product of the samples of composition 1 with temperature.

Fig. 8. Disproportionation peaks of two compositions of sintered NdFeB processed at 2000 mbar hydrogen.

Fig. 7. Demagnetisation curves in "Easy" and "Hard" directions for sample of composition 1 processed at 880 °C.

Fig. 9. Demagnetisation curve for HDDR processed sample of Composition 2 showing easy and hard direction of magnetisation.

Fig. 6 shows that the coercivity of the samples follows a smooth curve, peaking at 880 °C with a value of 840 ($\pm$ 0.17) kA m^{-1}, the remanence also reaches a maximum at this temperature but with a much sharper peak with a value of 1.08 ($\pm$ 0.02) T. The demagnetisation quadrant for this sample is shown in Fig. 7 together with the difference between the curve in the easy and in the hard direction of magnetisation, indicating significant anisotropy.

The relationship between magnetic properties and temperature exhibited a sharp peak in remanence and maximum energy product after treatment at 880 °C. These magnetic properties are certainly acceptable for a powder for use in bonded magnets. However, it should be noted that scaling-up the processing to much larger batches could cause issues with temperature control and with the kinetics of the HDDR reaction and would therefore require further work in order to establish the precise processing conditions and hence commercial viability of this process.

Further studies at 880 °C have shown that increasing the disproportionation pressure to 2000 mbar for composition 1 reduced the remanence to 0.72 ($\pm$ 0.02) T but retained the coercivity at 840 ($\pm$ 0.17) kA m^{-1} producing a maximum energy product of 85 ($\pm$ 2.0) kJ m^{-3}. This reduction in remanence and hence maximum energy product can be attributed to over-processing which occurs by taking the sample to a higher pressure than that required after the sample has completed the disproportionation reaction. It has also been shown that samples of composition 2 can be processed at 2000 mbar. Fig. 8 shows the comparison of the disproportionation peak of this sample (labelled "Composition 2") compared to that of the material described in the earlier part of this paper (labelled "Composition 1").
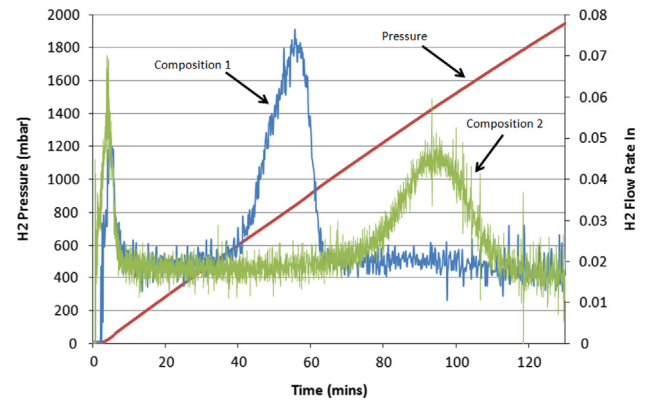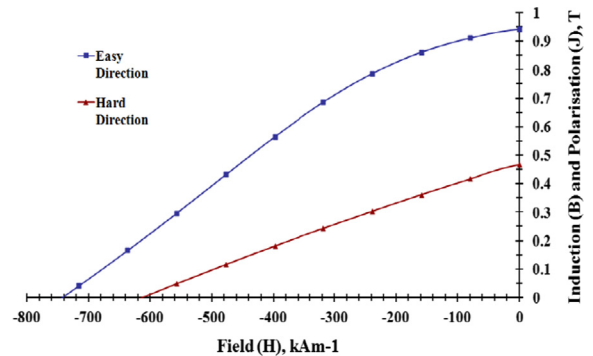
Fig. 8 shows that the sample with composition 2 starts and finishes its disproportionation reaction at a much higher pressure than that of composition 1. However, they both achieved completion in the pressure ramp stage up to 2000 mbar. These studies indicate that the increased presence of dysprosium and the addition of cobalt, increases the equilibrium pressure required for disproportionation, with a disproportionation start point, at 1110 mbar, and a finish point of 1750 mbar at 880 °C. This is significantly higher than the values reported for composition 1 which contains a relatively small amount of Dy and no Co.

The demagnetisation curve of the sample with composition 2 processed at 2000 mbar is shown in Fig. 9. This sample exhibits excellent anisotropy, with a coercivity of 740 kA m^{-1}, a remanence of 0.94 T and a maximum energy product of 117 kJ m^{-3}. As expected, these magnetic properties are lower than those of the initial sintered starting material.

Furthermore, it has been shown that mixed batches of samples with the two compositions could be co-processed successfully, giving rise to the possibility of processing mixed input feeds. Fig. 10 shows the disproportionation absorption peaks observed by processing a 50:50 mix of samples with composition 1 and 2 in one batch during the ramp stage to 2000 mbar at 880 °C.

Fig. 10 shows that the single mixed sample exhibited a combination of the absorption peaks from both of the individual compositions and the disproportionation reactions are complete within the ramping-up stage. This demonstrates that it is possible to process mixed batches of material using one set of processing conditions. The disadvantage of processing in this way is that some compositions will be subject to over-processing leading to lower magnetic properties compared to those of pre-separated compositions with individually designed processing conditions.
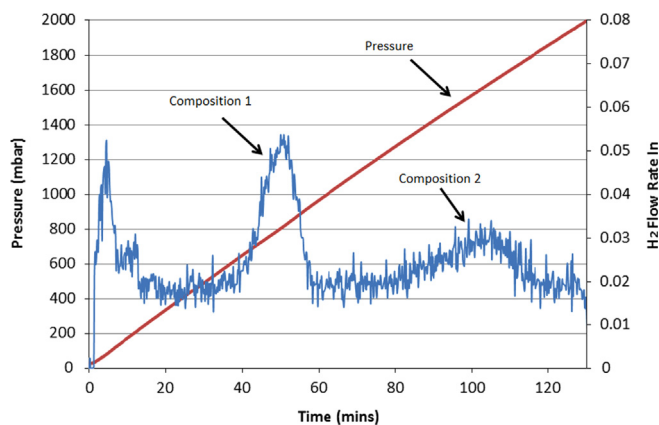
Fig. 10. Disproportionation peaks of a 50:50 mix of sample with Compositions 1 and 2 processed simultaneously in one batch.

4. Conclusions

Conducting the HD and HDDR processes in the same vessel lowers, by around 21%, the hydrogen pressure required for the initiation of disproportionation and gives improved magnetic properties by inhibiting the formation of $Nd_2O_3/Nd(OH)_3$ at the grain boundaries of the HD powder. It also provides powder much more suitable for subsequent hot compaction.

For samples with Composition 1, the best magnetic properties were achieved after processing at 880 °C, producing a sample with a magnetic remanence value of 1.08 (± 0.02) T and an intrinsic coercivity of 840 (± 17) kA m^{-1}. This represents an increase of 40 kA m^{-1} in the intrinsic coercivity compared to that reported previously [20], whilst maintaining a good remanence value. Disproportionation peaks are broadened with a lower peak height as the processing temperature is increased, indicating the increased stability of the $Nd_2Fe_{14}B$ phase at higher temperatures.

Magnets of mixed composition can be processed simultaneously by increasing the hydrogen pressure to allow full disproportionation.

Real scrap sources will contain magnets with a range of compositions and could therefore require a generic set of processing conditions. This paper has begun to address the processing conditions but further work is required in this area in an attempt to define the optimum processing conditions for particular mixtures.

References

[1] J.J. Croat, J.F. Herbst, R.W. Lee, FE. Pinkerton, Journal of Applied Physics 55 (1984) 2083.
[2] H. Onodera, Y. Yamaguchi, H. Yamamoto, M. Sagawa, Y. Matsuura, H. Yamamoto, Journal of Magnetism and Magnetic Materials 46 (1984) 151–156.
[3] M. Zakotnik, I.R. Harris, A.J. Williams, Journal of Alloys and Compounds 469 (2009) 314–321.
[4] S. Rivoirard, J.G. Noudem, P. de Rango, D. Fruchart, S. Liesert, J.L. Sobeyroux, Proceedings of the 16th International Workshop on Rare Earth Magnets and their Applications, Japan, 2000, p. 355.
[5] University of Birmingham, UK Patent Application no. 1020383.4, December 2010.
[6] A. Walton, A.J. Williams, Recycling International, May 2011.
[7] A. Walton, Han Yi, V.S.J. Mann, A.I. Bevan, J.D. Speight, I.R. Harris, A.J. Williams, Proceedings of the 21st International Workshop on Rare-Earth Magnets and Their Applications, Nagasaki, 2012, pp. 10–13.
[8] A. Walton, A.J. Williams, Materials World, August 2011.
[9] P.J. McGuinness, E.J. Devlin, I.R. Harris, E. Rozendaal, J. Ormerod, Journal of Materials Science 24 (1989) 2541.
[10] T. Takeshita, R. Nakayama, Proceedings of the 10th International Work-shop on Rare Earth Magnets and their Applications, Kyoto, 1989, p. 551.
[11] P.J. McGuinness, X.J. Zhang, X.J. Yin, I.R. Harris, Journal of Less Common Metals 158 (1990) 359.
[12] T. Takeshita, R. Nakayama, Proceedings of the 12th International Workshop on Rare Earth Magnets and their Applications, Canberra, 1992, p. 670.
[13] I.R. Harris, Proceedings of the 12th International Workshop on Rare Earth Magnets and their Applications, Canberra, 1992, p. 347.
[14] S. Sugimoto, O. Gutfleisch, I.R. Harris, Journal of Alloys and Compounds 260 (1997) 284.
[15] M. Zakotnik, A.J. Williams, I.R. Harris, Proceedings of the 18th International Workshop on High Performance Magnets and their Applications, Annecy, 2004, pp. 267–274.
[16] D. Kim, J. Yu, J. Lee, T. Jang, T. Lim, Proceedings of the 21st International Workshop on Rare Earth Magnets and their Applications, Slovenia, 2012, p. 242–244.
[17] Y. Honkura, C. Mishima, N. Hamada, G. Drazic, O. Gutfleisch, Journal of Magnetism and Magnetic Materials 290–291 (1990) 1282–1285.
[18] H. Nakamura, K. Kato, D. Book, S. Sugimoto, M. Okada, M. Homma, Proceedings of the 15th International Workshop on Rare Earth Magnets and their Applications, Dresden, 1998, pp. 507–516.
[19] S. Sugimoto, H. Nakamura, K. Kato, D. Book, T. Kagotani, M. Okada, M. Homma, Journal of Alloys and Compounds 293–295 (1999) 862–867.
[20] R.S. Sheridan, R. Sillitoe, M. Zakotnik, I.R. Harris, A.J. Williams, Journal of Magnetism and Magnetic Materials 324 (2012) 63–67.
[21] O. Gutfleisch, K. Guth, T.G. Woodcock, L. Schultz, Advanced Energy Materials 3 (2) (2013) 151–155.
[22] R.S. Sheridan, A.J. Williams, I.R. Harris, A. Walton, Proceedings of the 22nd International Workshop on Rare-Earth Permanent Magnets and their Applications, 2012, pp. 394–397.
[23] A.J. Williams, P.J. McGuiness, I.R. Harris, Journal of the Less Common Metals 171 (1991) 149–155.
[24] J.P. Meakin, J.D. Speight, I.R. Harris, A.J. Williams, M.P. Taylor, A. Walton, Proceedings of the 22nd International Workshop on Rare-Earth Permanent Magnets and their Applications, 2012, pp. 399–402.
[25] I.R. Harris, A.J. Williams, Grain Boundaries: Their Character, Characterisation and Influence on Properties, 165–185.